

# Modelling and performance evaluation of a direct steam generation solar power system coupled with steam accumulator to meet electricity demands for a hospital under typical climate conditions in Libya

Amin Ehtiwesh, Cagri Kutlu<sup>\*</sup>, Yuehong Su, Saffa Riffat

Department of Architecture and Built Environment, Faculty of Engineering, University of Nottingham, University Park, Nottingham, NG7 2RD, UK

## ARTICLE INFO

### Keywords:

Demand profile  
Direct steam generation Rankine Cycle  
Operation control  
Simulink/Simscape  
Steam accumulator

## ABSTRACT

This study aims to build a dynamic model of a direct steam generation (DSG) solar power system coupled with a steam accumulator to meet electricity demands for a hospital under transient environmental conditions in Libya. The main components of the system are DSG parabolic trough collectors, a steam accumulator, a turbine, a condenser and a circulation pump. The system is modelled via using Simulink/Simscape software blocks with integrated MATLAB functions to run a dynamic simulation. As the simulation tool reflects the transient operation of the components, advanced control strategies were applied to the model. Using the proportional integral controller (PI controller), safe operation of the system is secured by pump flow rate control, safe turbine operation is provided by pressure control and power output is matched with the demand by using a throttle valve control. 1584 m<sup>2</sup> solar collector area and 160 m<sup>3</sup> total volume of pressurized steam tank are used in the simulation considering the electricity demand of the hospital and solar radiation in the location. The produced work output was controlled to match the demand profile of the hospital, which needs 200 kW in the peak period and 50 kW at the night. The designed system shows a maximum thermal efficiency of 23.5% for the operation condition.

## 1. Introduction

Solar thermal power generation plays an important role in renewable electricity production. At present, there is a rapid increment of using this kind of technology [1]. Up to date, the global installed solar electricity generation systems reached up to 6200 MW, with another 1250 MW under construction using different types of solar collectors. Commercial solar power generation systems based on parabolic trough collectors have proven to be the most mature and prevalent, accounting for over 90% of the total capacity of operating and under-construction facilities. Solar thermal energy systems are utilized not just for power generation, but also for a variety of energy-intensive systems such as desalination, hot domestic water synthesis, refrigeration, and pharmacology industrial [1]. Recently, electricity is the most important energy source for different uses especially in hospitality and health sector in the world. Electricity can be used to power all devices in hospitals, and it is the most demanded energy. However, there is a real problem in southwest Libya for supplying electricity demands for many sectors during the day

[2]. Although there is a diesel generator for each hospital and public buildings, the shutdown of electricity is still going on, which causes problems in the operation department at the hospitals [3].

As a sustainable and reliable solution to this weak grid setting in order to provide enough electricity for hospital operations, direct steam generation solar power systems based on parabolic trough collectors can be considered as an alternative and good option [4]. Therefore, direct steam generation solar power system driven by PTC technology has been widely examined [5]. The steam is generated directly in solar collector fields without needing to use an auxiliary boiler, which results in reducing and avoiding the use of an additional pump and its consumption and heat losses. In the evaporation region of water, the collectors benefit from the constant temperature and high coefficient of heat transmission [6]. As an application, Abengoa solar company built a solar energy plant with 8 MWh capacity. This solar plant has two separate regions, an evaporator field with three loops and two loops for superheater region to reach at 450 °C and 8.5 MPa [7]. An innovative control strategy of system has guaranteed the stability of the plant under cloudy climate conditions for one year of operation. Moreover, evaluation of

<sup>\*</sup> Corresponding author.

E-mail addresses: [Amin.Ehtiwesh@nottingham.ac.uk](mailto:Amin.Ehtiwesh@nottingham.ac.uk) (A. Ehtiwesh), [cagri.kutlu2@nottingham.ac.uk](mailto:cagri.kutlu2@nottingham.ac.uk) (C. Kutlu), [yuehong.su@nottingham.ac.uk](mailto:yuehong.su@nottingham.ac.uk) (Y. Su), [saffa.riffat@nottingham.ac.uk](mailto:saffa.riffat@nottingham.ac.uk) (S. Riffat).

<https://doi.org/10.1016/j.renene.2023.02.075>

Received 24 November 2022; Received in revised form 29 January 2023; Accepted 17 February 2023

Available online 19 February 2023

0960-1481/© 2023 The Authors. Published by Elsevier Ltd. This is an open access article under the CC BY license (<http://creativecommons.org/licenses/by/4.0/>).

Nomenclature		$\rho$	density, $\text{kg m}^{-3}$
$A$	Area, $\text{m}^2$	$\nu_v$	The specific volume of the vapor
$C_p$	Specific heat, $\text{J kg}^{-1}\text{K}^{-1}$	$\nu_L$	The specific volume of the liquid
$G$	Solar irradiance, $\text{W m}^{-2}$	$\nu_R$	The specific volume at the restriction aperture
$h$	Enthalpy, $\text{kJ}$	<i>Subscripts</i>	
$\dot{m}$	Mass flow rate, $\text{kg s}^{-1}$	am	Ambient
$M$	Mass, $\text{kg}$	in	Inlet
$P$	Pressure, $\text{MPa}$	out	Outlet
$\dot{Q}$	Rate of heat transfer, $\text{kW}$	mean	mean temperature
$T$	Temperature, $^{\circ}\text{C}$	s	Steam
$U$	Overall heat transfer coefficient, $\text{W m}^{-2}\text{K}^{-1}$	<i>Abbreviation</i>	
$V$	Volume, $\text{m}^3$	PTC	Parabolic trough collector
$\dot{W}$	Power output, $\text{kW}$	DSG	Direct steam generation
$Z_L$	Liquid volume fraction	HTF	Heat transfer fluid
$F_M$	Mass fraction of the liquid	ORC	Organic Rankine cycle
$S_R$	The flow area of the restriction aperture	TES	Thermal energy storage
<i>Greek letters</i>		DHW	Domestic hot water
$\eta$	Efficiency		

different configurations of interconnections between flexible rotation joints, solar collectors and ball joints has been done [8]. The first commercial direct steam generation 5 MWe solar thermal power plant driven by PTC technology has been established in Kanchanaburi/Thailand. It uses modern a PTC system made of composite material combined with an efficient thin-glass mirror which reflects more than 95% of the sun radiation. The plant works under clear and cloudy climate conditions, but under cloudy conditions, it requires high control of PTC loops [9]. Although direct steam generation solar power system driven by PTC technology uses turbine-based steam Rankine cycle for thermal power generation have many advantages, there are some disadvantages using this system as follows: Firstly, only allowing a suitable high pressure range level and the superheated steam generation to enter the turbine to overcome condensation of vapor during the expansion process when heat sources decreased [10]. If the vapor is condensed and enters to

steam turbine, it may touch on the blades of turbine at high speed and will damage the turbine [11]. Secondly, large direct steam generation solar power plants are more economic than small capacity one [12], where the capital cost per kW of a solar electricity generation system generally decreases with the increment in installed capacity [13]. Direct steam generation solar power plants can generate from a few hundred kW to more than 200 hundred MW [14]. Finally, it is not easy to store high-grade heat to be used later [15]. The stored heat is necessary to drive the thermal plant when solar irradiance is very weak or during night. Regarding to control of power output, Kutlu et al. [16] designed a solar-ORC integrated with pressurized hot water storage unit for community level application, their results matched the demand profile of the twelve houses. Aghaziarati et al. [17] modelled a combined cooling, heating and power system based on solar-ORC and cascade refrigeration cycle to provide electricity, hot water and cooling to a hospital in Iran.

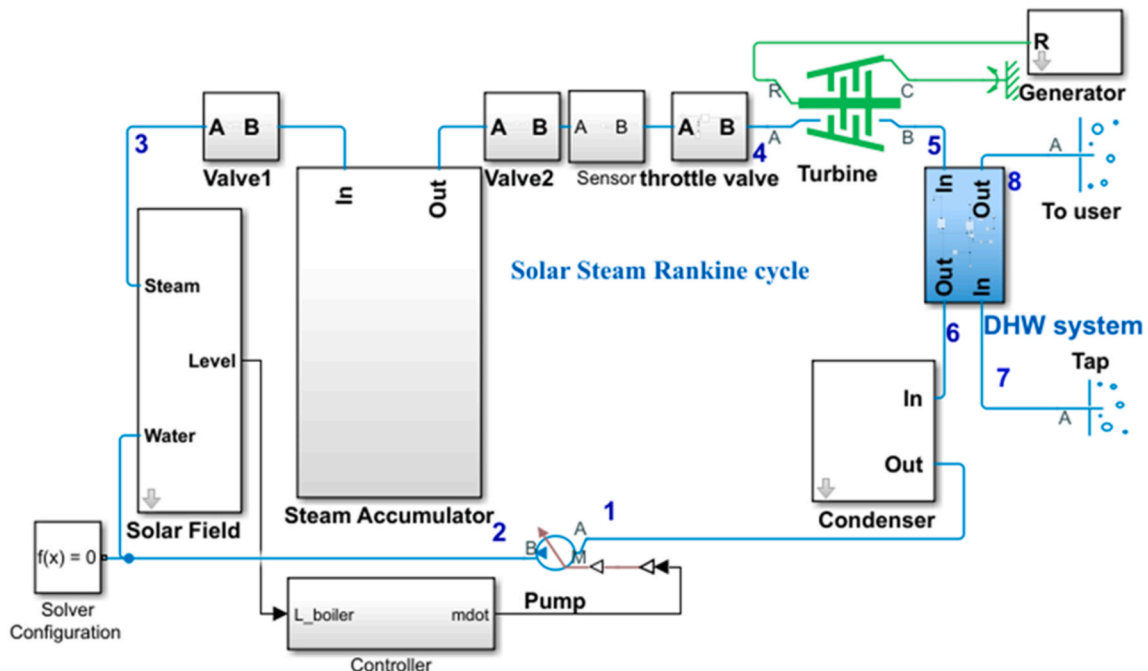


Fig. 1. The layout of the DSG solar power system coupled with steam tank in Simulink\Simscape software.

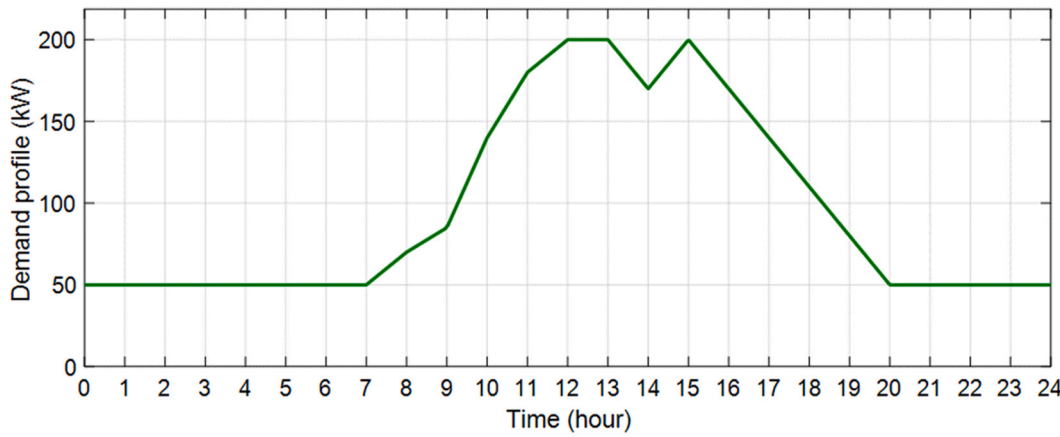


Fig. 2. Libya Murzuq general hospital’s daily electricity usage profile [21].

Pina et al. [18] proposed of a PTC-ORC–Biomass cooling plant for a commercial centre, they achieved good results to reducing based on fuel energy. Arteconi et al. [19] modelled on system integration of a micro solar-ORC plant to supplies energy for a residential building. The results showed the convenience of the proposed system especially when it operates in trigeneration mode, which allows better exploitation of the

thermal energy produced in the summer.

The above issues can be solved or eased by using a control strategy regarding adopting a throttle valve at the inlet of the turbine to control pressure. To produce electricity on the condition of large temperature differences or weak solar irradiances, a steam accumulator as a heat storage tank is one of the best solutions in direct steam generation solar

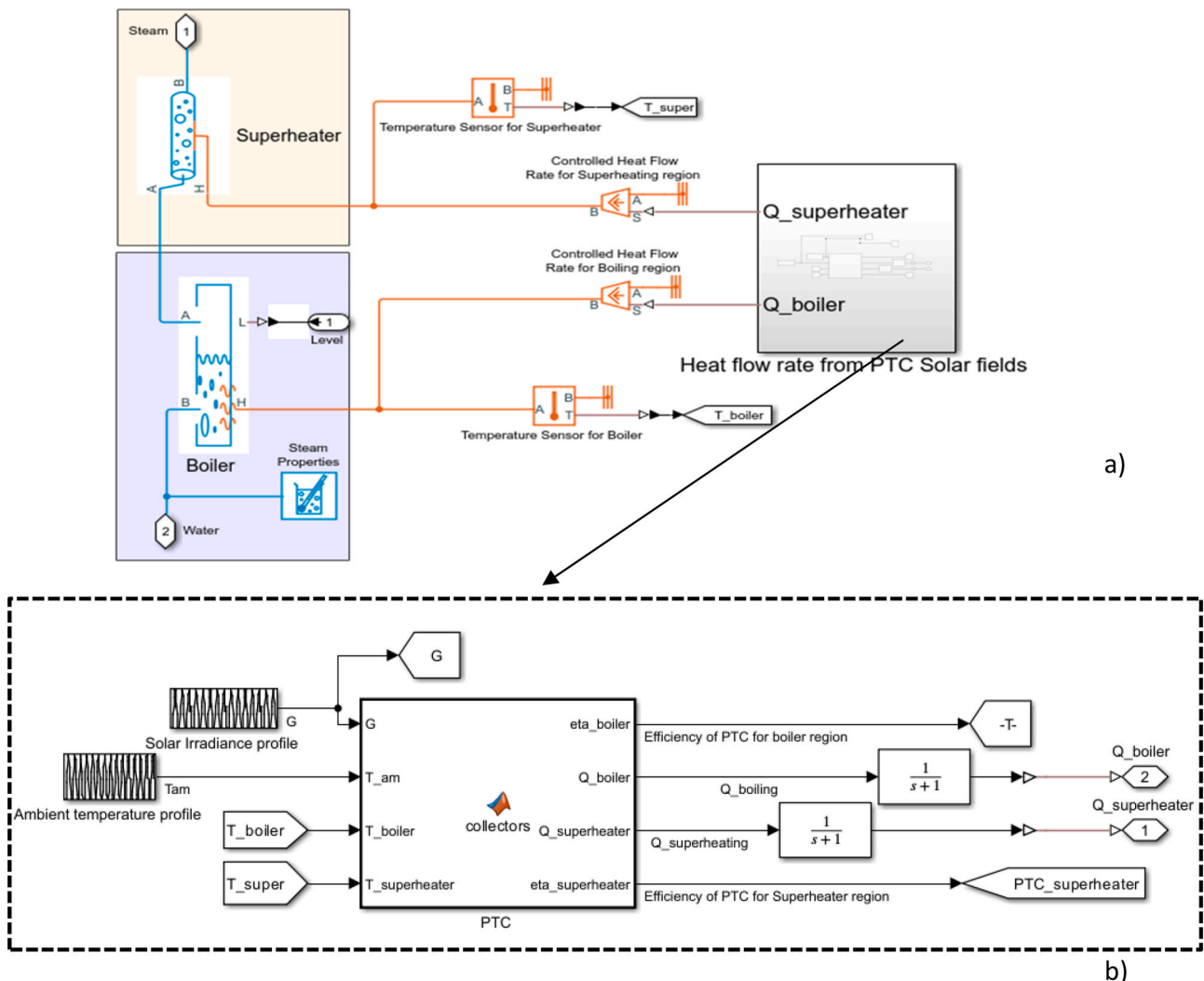


Fig. 3. (a) Simulink\Simscape blocks of the solar field; (b) MATLAB function input and output signals.

power systems. Direct steam generation solar power system will be more beneficial than solar indirect steam generation system [20]. To the best of the authors' knowledge, investigation of direct steam generation solar power systems is still a subject for further study, particularly in the field of heat exchangers design, heat storage tanks with advanced control methodologies in order to secure the safe operation, maximum yield and demand-based operation. Therefore, in this paper, a novel direct steam generation solar power system integrated with a steam accumulator is proposed. The system is dynamically modelled to meet the electricity and domestic hot water demand of a hospital in southwest Libya under typical climate conditions via using Simulink\Simscape software.

## 2. Description of the system

The proposed direct steam generation (DSG) solar Rankine cycle supplies electricity and domestic hot water (DHW) for a hospital in Libya. Its schematic layout in Simulink\Simscape block diagrams is presented in Fig. 1. The system comprises of PTCs in solar field, a steam accumulator, a throttle valve, steam turbine, a heat exchanger which is used in the DHW production process in this system, a water drum condenser and a pump. The overall analysis of the proposed system is simulated on Simulink\Simscape software. A liquid drum condenser has been chosen in this study to accumulate the exhaust steam from the turbine. The volume of this liquid drum is 0.48 m<sup>3</sup> as a design condition. A and B are the ports of a block, R is mechanical rotational conserving port with shaft and C is casing.

The water enters the pump as a saturated liquid '1' at condensing pressure, then its pressure is increased by pump to the evaporating pressure level '2'. Evaporating pressure depends on the solar radiation level and the flow rate strategy. In the solar field, there are boiler and superheater regions, at the outlet of the superheater, the fluid phase is superheated steam '3'. Then the saturated steam flows into the turbine at point '4', exporting power during the process of enthalpy drop. The exhausted steam from the turbine enters to the DHW heat exchanger at point '5' and then it loses heat and enters to condenser unit at point '6' and leaves as condensed water.

There can be two operating modes for the system:

**Mode (I):** The system needs to generate electricity and solar radiation is abundant. In this mode, Valve 1 and Valve 2 are open, and the pump runs. Both DSG and DHW operate during this mode. The working fluid water is heated and vaporized in the Solar field with PTCs. The saturated steam flows into the steam accumulator and turbine, exporting power during the process of enthalpy drop. The outlet vapor is condensed to saturated liquid in DHW system and in the condenser. The extracted heat by the heat exchanger in DHW system is used to heat up the water for end-users. The condensed working fluid is pressurized by the pump and then is sent back to the solar field.

**Mode (II):** The system needs to generate electricity and DHW, but irradiation is unavailable. Valve 2 is open, and Valve 1 is close. The heat is released by the steam accumulator and converted into power. Condensed water is accumulated in the condenser liquid drum.

## 3. Hospital energy requirements

The southwest Libyan hospital Murzuq General Hospital's average electricity and hot water needs must be met by the proposed system. The hospital has 120 beds and an overall size of 8,000 m<sup>2</sup> [21]. Due to the constant need for hot water in the pharmacy, laboratory, and other facilities, the electricity consumption for air conditioning, lighting, and medical equipment can reach 200 kW. In this simulation, there is typical day taken into account. Fig. 2 shows the hospital's daily electricity usage profile. The hospital operates full-time and every day of the year. The electricity demand starts to increase around 7:00 a.m. and then decreases after 3:00 p.m. Given that only the emergency department is open at night and that all other departments are closed, it is clear that demand is higher during the daytime and lower during the night. From

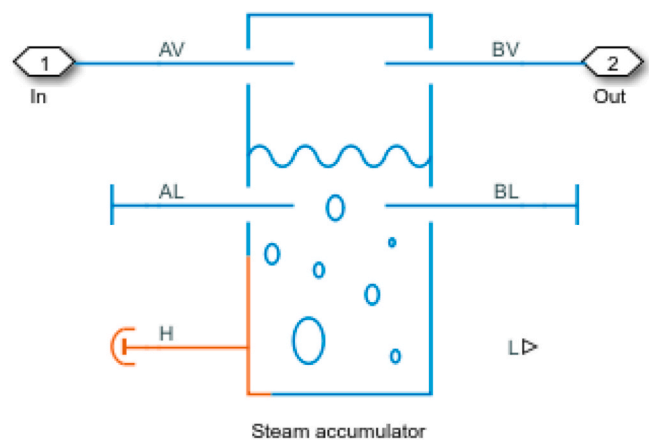


Fig. 4. Steam accumulator block in Simscape.

8:00 p.m. to 7:00 a.m., the electricity demand remains constant at 50 kW.

## 4. Mathematical models

### 4.1. Solar field model

The model of the solar field is based on separation of the collectors as boiler and superheater sections. 97.3% of the collectors are used in the boiler section and the remaining 1.7% are used as superheater. Boiler section has 118 modules, and superheater section has 2 modules. Each module has a total area of 13.2 m<sup>2</sup> [22]. These numbers are used for calculation of useful heat input in collector model. In Simulink\Simscape environment, saturated fluid chamber (a steam drum) is used as boiler section and two-phase fluid pipe is used as superheating region as seen in Fig. 3a. Both elements have controlled heat flow rate sources to operate as solar heat input which is calculated by MATLAB function block. Boiler section has liquid level signal which is used to control flow rate. In this way, same liquid level can be kept in the boiler and flow rate is controlled. The heat flow rate signals to the heat source elements come from the second block which is shown in Fig. 3b. The collector equations are written in the MATLAB function block using mean temperature in the collector, solar radiation and ambient temperature.

As solar collectors, concentrated type is chosen for this study. Industrial Solar Technology (IST-PTC) collector is chosen which is high efficiency parabolic trough collector and it has been already evaluated for its potential in DSG solar power systems [23]. The reasons for selecting this kind of concentrated solar collector are its low cost, easy ability to be installed even on building roofs and its proven performance. The thermal performance formula of a single PTC provided by the manufacturer is given in Eq. (1) [24].

$$\eta_{PTC} = 0.762 - 0.2125 \times \frac{T_{in} - T_{am}}{G} - 0.001672 \times \frac{(T_{mean} - T_{am})^2}{G} \quad (1)$$

where here  $G$  is solar irradiance,  $T_{am}$  is ambient temperature.  $T_{in}$  is inlet collector temperature and  $T_{mean}$  is mean temperature and it can be expressed by Eq. (2)

$$T_{mean} = \frac{T_{in} + T_{out}}{2} \quad (2)$$

$T_{out}$  indicates solar collector outlet temperature. Solar Rankine cycles often require hundreds of collectors, and the temperature differential between adjacent collectors is intended to be minimal. When determining the overall collection efficiency, it is appropriate to assume that the average operating temperature of the collector fluctuates continuously from one module to the next. The amount of solar radiation absorbed by the solar collectors is equal to the enthalpy increase of the

steam and it can be expressed by Eq. (3).

$$\dot{Q}_{solar} = G \cdot A_{PTC} \cdot \eta_{PTC} = \dot{m}_{water} (h_3 - h_2) \tag{3}$$

Here  $A_{PTC}$  indicates total area of the solar collectors,  $\dot{m}_{water}$  is mass flow rate of water,  $h_2$  and  $h_3$  are inlet and outlet enthalpies of working fluid.

In order to solve given equations, MATLAB function uses input signals as shown in Fig. 4b. Solar irradiance and ambient temperature profiles are given boiler and superheater temperature signals are taken from the solar field, these temperatures are used for calculation of thermal efficiency of the collectors. Outputs of the equations are thermal efficiencies of boiler and super heater sections and heat outputs. Calculated heat outputs are connected to boiler and super heater elements.

#### 4.2. Steam accumulator model

One of the important components in the proposed system is the steam accumulator because it is used as the heat source for the Rankine cycle during discharging mode, and it is used for separating the liquid and steam before it enters to turbine [25]. Steam accumulators are used as a thermal storage unit in several industries [26]. Their excellent ramp/response time and energy storage capabilities are the main reasons for their extensive use. During a vessel's charging cycle, a standard system uses steam accumulators to hold a water-steam mixture, pressurising the steam at the top of the vessel [27,28]. The combination reaches saturation and stabilises there throughout charging. When the discharge valve is opened, the steam exits the vessel. Pressure and saturation temperature drop as the discharge cycle goes on, flashing more liquid to steam that eventually discharges as well. Steam accumulators only create saturated steam at sliding pressures, despite having the ability to release steam quickly and having round-trip efficiency of 60–80%. Its energy capacity, which is related to its volume, determines the energy storage level in the system. The volume of steam accumulator can be calculated by Eq. (4) [25].

$$V_{steel} = V_{steam} = \frac{3600t_H \cdot \dot{W}_{net}}{\rho_s \cdot \eta_{sys} \cdot C_p_s \cdot \Delta T} \tag{4}$$

Where  $V_{steam}$  is the steam volume,  $t_H$  is storage time in hour,  $C_p_s$  is the heat capacity of steam and  $\Delta T$  is the temperature drop in discharging process. The layout of steam accumulator block in Simulink\Simscape is shown in Fig. 4.

For steam accumulator, two phase receiver accumulator block is used in the Simulink\Simscape. Its model is based on some assumptions: The steam storage wall is assumed as rigid and adiabatic, so heat loss to the ambient is neglected and total volume of the container is constant. Pressure is always below the critical pressure, the hydrostatic pressure in the container is neglected. Liquid and vapor masses are considered separately, mixture is not modelled and finally, the pressure losses through the output port are zero. Also, in this study, only vapor inlet and outlet are operating, there is no liquid flow in and out.

The liquid volume fraction of the tank is expressed by Eq. (5)

$$Z_L = \frac{f_{M,L} \nu_L}{f_{M,L} \nu_L + (1 - f_{M,L}) \nu_v} \tag{5}$$

$f_{M,L}$  is the mass fraction of the liquid.  $\nu_L$  is the specific volume of the liquid.  $\nu_v$  is the specific volume of the vapor. When the liquid specific enthalpy is greater than or equal to the saturated liquid specific enthalpy, the mass flow rate of the vaporizing fluid is determined from Eq. (6)

$$\dot{m}_{vap} = \frac{M_L (h_L - h_{L,sat})}{\tau (h_v - h_{L,sat})} \tag{6}$$

$M_L$  is the total liquid mass.  $h_L$  is the specific enthalpy of the liquid at the internal node.  $h_{L,sat}$  is the saturated liquid specific enthalpy at the in-

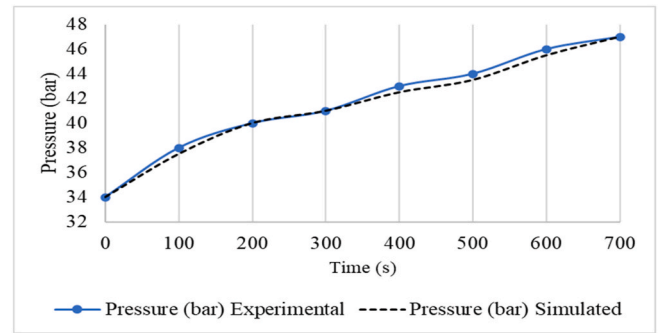


Fig. 5. Measured [29] and calculated pressure in the steam accumulator.

ternal node.  $h_v$  is the specific enthalpy of the vapor.  $h_{v,sat}$  is the saturated vapor specific enthalpy.  $\tau$  is the vaporization and condensation time constant parameter. The energy flow linked to vaporization is as follows:

$$\dot{Q}_{vap} = \dot{m}_{vap} h_{v,sat} \tag{7}$$

The total accumulator volume is constant. Due to phase change, the volume fraction and mass of the fluid changes. The mass balance in the vapor zone is calculated by Eq. (8) [29].

$$\frac{dM_v}{dt} = \dot{m}_{v,in} - \dot{m}_{v,out} + \dot{m}_{con} - \dot{m}_{vap} \tag{8}$$

$M_v$  is the total vapor mass.  $\dot{m}_{v,in}$  is the inlet vapor mass flow rate at all liquid and vapor ports.  $\dot{m}_{v,out}$  is the outlet vapor mass flow rate and it is written by Eq. (9)

$$\dot{m}_{v,out} = -(\dot{m}_{v,inlet} - \dot{m}_{v,outlet}) \tag{9}$$

The energy balance in the vapor zone is determined by Eq. (10)

$$M_v \frac{du_v}{dt} + \frac{dM_v}{dt} u_v = \dot{Q}_{vap,in} - \dot{Q}_{vap,out} - \dot{Q}_{con} + \dot{Q}_{vap} + \dot{Q}_{vh} \tag{10}$$

$u_v$  is the specific internal energy of the vapor.  $\dot{Q}_{vap,in}$  is the inlet vapor energy flow rate at all liquid and vapor ports.  $\dot{Q}_{vh}$  is the heat transfer between the tank wall and the vapor.

As steam accumulator is one of main important part in this study, the validation part is necessary to validated simulation results for a test of steam accumulator charging mode. The experimental data of pressure variations inside the charging steam accumulator of Stevanovic et al. [29] are used to simulate and analyse charging and discharging transients in the horizontal cylindrical steam accumulator, which has an outside length of 11.9 m, an outer diameter of 2.9 m, and a total internal volume of 64 m<sup>3</sup>. The operating range for the accumulator is 25–55 bars. The steam headers at the top of the interior of the accumulator vessel are where steam is fed into the accumulator through the perforated tubes that are immersed in the water volume. In each simulation run, it is assumed that water and steam are in a state of thermal equilibrium caused by the initial pressure.

Steam accumulator was thermodynamically validated. The best agreement of the calculated pressure transient with the measured data is obtained by the application of the nonequilibrium model. Through direct comparisons between pressure development from the simulation and the data taken from Ref. [29], the performance of the system has been validated. The case depicts how a steam accumulator is charged. The comparison of simulated and experimental pressures is shown in Fig. 5. The pressure growth nearly aligns the referred one and it satisfies the required standards.

#### 4.3. Throttle valve model

The throttle valve has been used here in this study to control steam

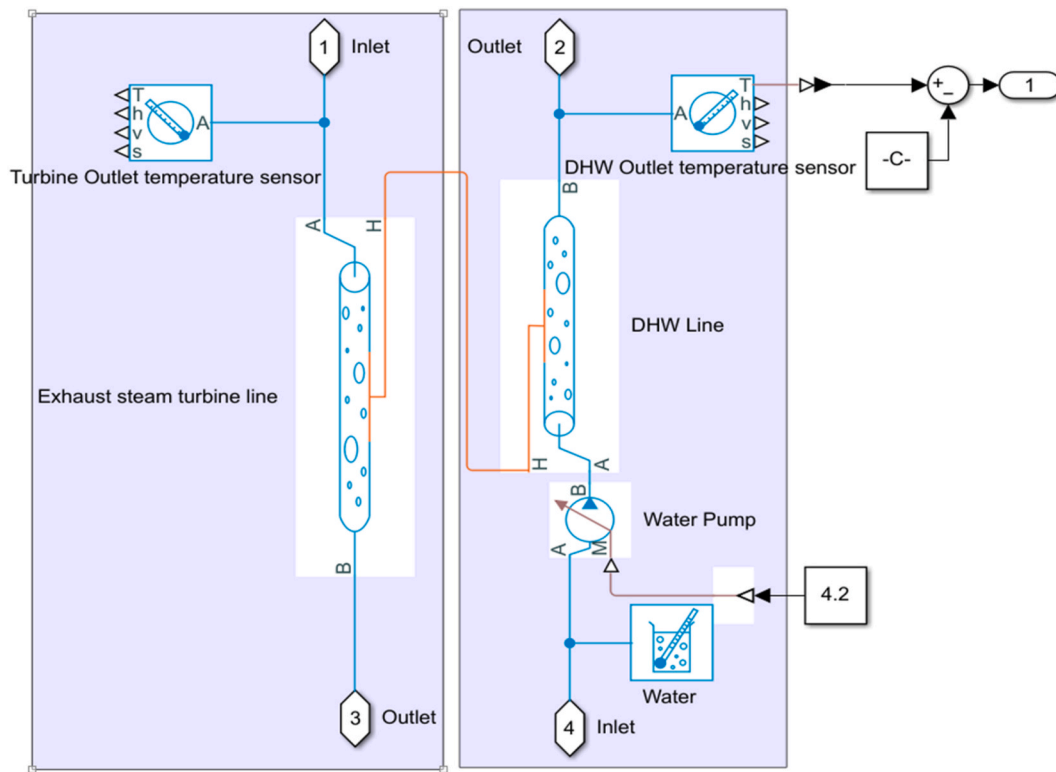


Fig. 6. Heat exchanger model for DHW heating.

flow rate before enters the steam turbine as it utilized to regulate flow of steam and gas in large, high-pressure pipelines, such as the main steam line serving a large, high-pressure turbine or a turboexpander gas supply line. The mass flow rate is based on Eq. (11) when the flow is turbulent [30]:

$$\dot{m} = S_R(P_{in} - P_{out}) \sqrt{\frac{2}{[P_{in} - P_{out}] \nu_R K_T}} \quad (11)$$

SR is the flow area of the restriction aperture and  $\nu_R$  is the specific volume at the restriction aperture. where  $K_T$  is defined as:

$$K_T = \left(1 + \frac{S_R}{S}\right) \left(1 - \frac{\nu_{in} S_R}{\nu_R S}\right) - 2 \frac{S_R}{S} \left(1 - \frac{\nu_{out} S_R}{\nu_R S}\right) \quad (12)$$

#### 4.4. Steam turbine

Steam turbine was chosen for the simulation due to well fitted and commonly used in the medium scale Rankine cycle systems. The steam is stored in the steam accumulators once the charging phase is through, making it ready to be used to produce electricity. Since the inlet mass flow rate, temperature, and pressure change throughout the discharging process, it is necessary to simulate the steam turbine's part-load behaviour in order to calculate its power output [31]. By Simulink \Simscape model, electrical output can be calculated. Moreover, this model gives the rotational speed of the turbine. Therefore, two-phase turbine block is used in the model. Usually, steam plants have high- and low-pressure turbines to expand high pressure steam to low pressure by considering turbines' pressure ranges. As this study uses one turbine,

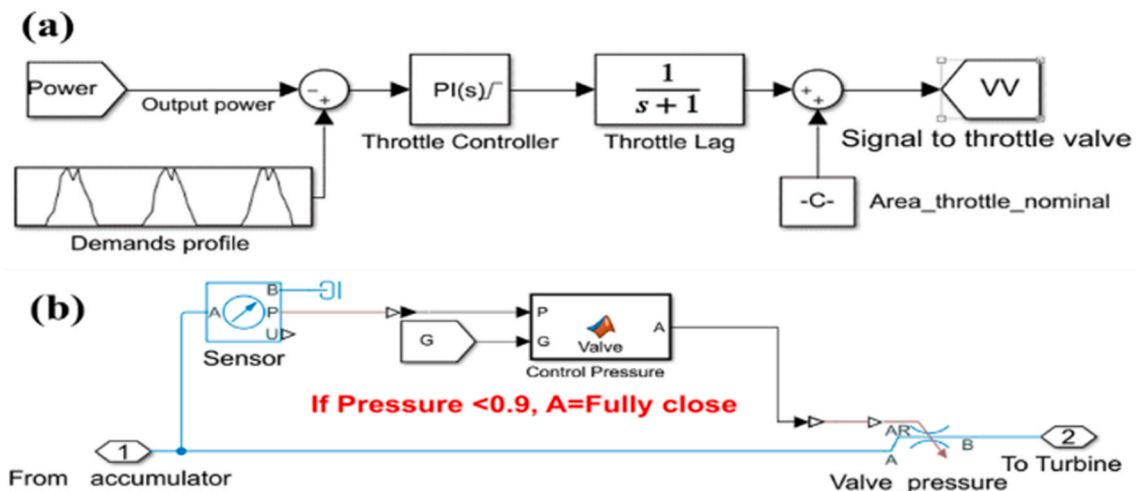


Fig. 7. Diagram control strategy of the system, a) To meet electricity profile, b) To ensure turbine inlet pressure.

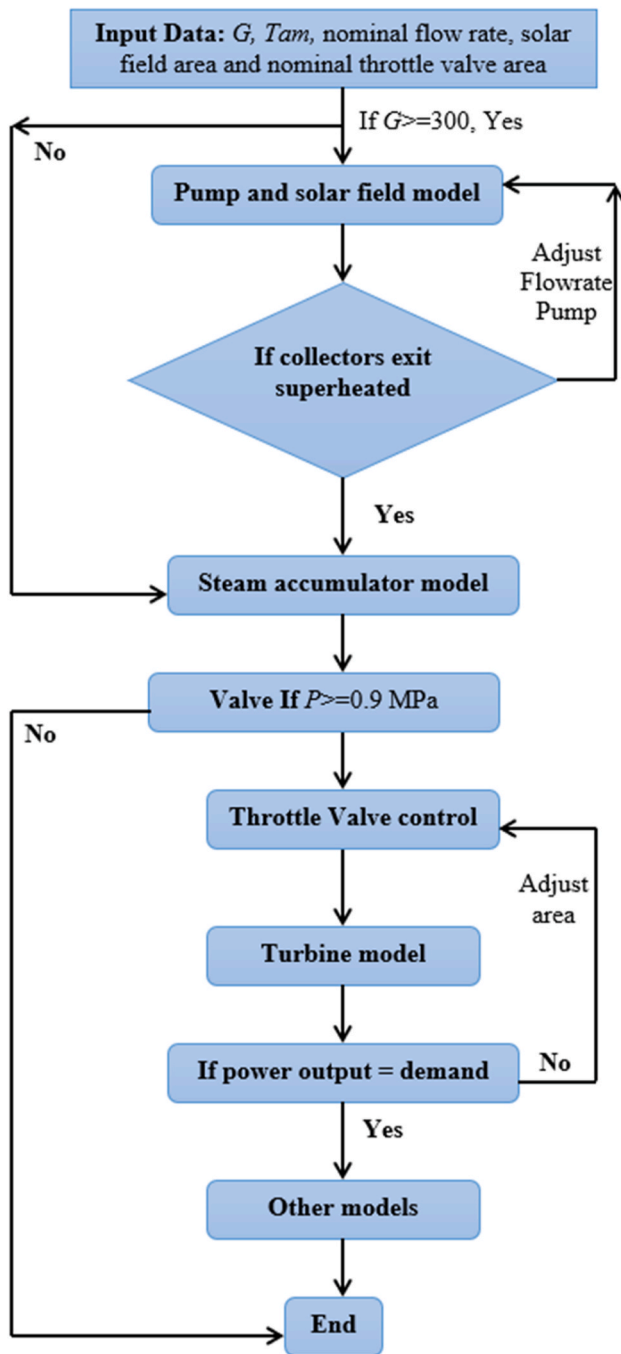


Fig. 8. Flow chart of work in this paper.

its inlet pressure is controlled to avoid lower operation pressures. The MAN power manufacturing business has advised that the lowest turbine inlet pressure should be 0.9 MPa [32,33]. Thus, this turbine’s minimum input pressure is set at 0.9 MPa.

4.5. DHW heat exchanger model

The exhaust steam at the turbine exit is directed to the heat exchanger where it is converted to the liquid state by rejecting its heat to the DHW system [34]. For this model, two two-phase pipe blocks have been connected each other to simulate heat transfer. In the model, thermal resistance between the tubes is neglected but the used blocks calculate the heat transfer coefficients inside the tubes based on flow rates and tube specifications [35]. Exhaust steam side temperature,

Table 1

Chosen parameters in the PTC-DSG solar power system.

Item	Value
Solar collector area (m <sup>2</sup> )	1584
Turbine isentropic efficiency	0.85
Isentropic efficiency of the pump	0.85
Efficiency of the Generator	0.95
Solar irradiance (W/m <sup>2</sup> )	350–1000
DHW outlet temperature (°C)	40–50
Ambient temperature (°C)	25–40
Steam accumulator volume (m <sup>3</sup> )	160
Length of DHW tube (m)	100
Tube inside/outside diameter (mm)	0.03/0.1

pressure and flow rate are based on the operation conditions during the day. However, DHW line uses constant flow rate which is given by hospital and the inlet temperature is tap temperature. Heat exchanger model in Simulink\Simscape for DHW heating schematic is given in Fig. 6.

4.6. Condenser drum

Water-cooled condenser is used in this study because it is mostly used in SRC systems which have access to consistent supply of water [36]. Similar to boiler in solar field, saturated fluid chamber is used for condenser. This time heat is rejected from the chamber and condensation is happened; all condensed water is moved to the pump if it is running. If the pump is off, condensed water is accumulated in the condenser until pump is switched on.

4.7. Control strategy of the system

The working fluid may reach the two-phase zone at the turbine inlet when the system is operating on a cloudy day because clouds can reduce irradiance. This may result in severe damage to the turbine blades due to the liquid impact, making the system output power unstable [28]. It is crucial to adopt a control strategy for the direct steam generation solar power system in order to make the system operate safely as well as to meet the electricity demand profile for one day. Therefore, a control system is adopted. Fig. 7a illustrates the system’s control method, which involves utilising a throttle valve before the turbine to regulate the flow rate in order to match the flow profile to the electricity demand profile for one day in a typical climate. Throttle valve or governor valve is a big valve at the inlet pipe of the turbine. It has the same size as inlet. After receiving a signal from governor, by using the actuator, the opening area of the valve will change. As the size of opening changes, certain amount of steam can pass the valve. The valve can be opened or closed to any desired flow by means of a motorized operator. In this model, the signal comes from the power output and second signal comes from demand profile, then these signals compared. Based on this difference, a new signal is sent by PI controller to the throttle valve for updating area opening according to desired flow value to match demand. Fig. 7b shows diagram of the turbine inlet pressure control strategy of the system.

The outline work of this study by using Simulink\Simscape software is shown in Fig. 8. First, the design conditions such as area of solar collectors, parameters and volume of steam accumulator was determined. The meteorological data of Murzuq city in Libya was added to the model by using EnergyPlus weather data [37] for a typical day in March. When solar irradiance is >= 300 W/m<sup>2</sup>, the valve is open, and pump runs. Water heats up to reach superheated state and charging the tank and then drives the turbine to produce electricity, and DHW from the condenser. Pressure control valve is set to be open if pressure is >= 0.9 MPa. Steam flows through the throttle valve and it is controlled according to a desired energy flow to match demand profile.

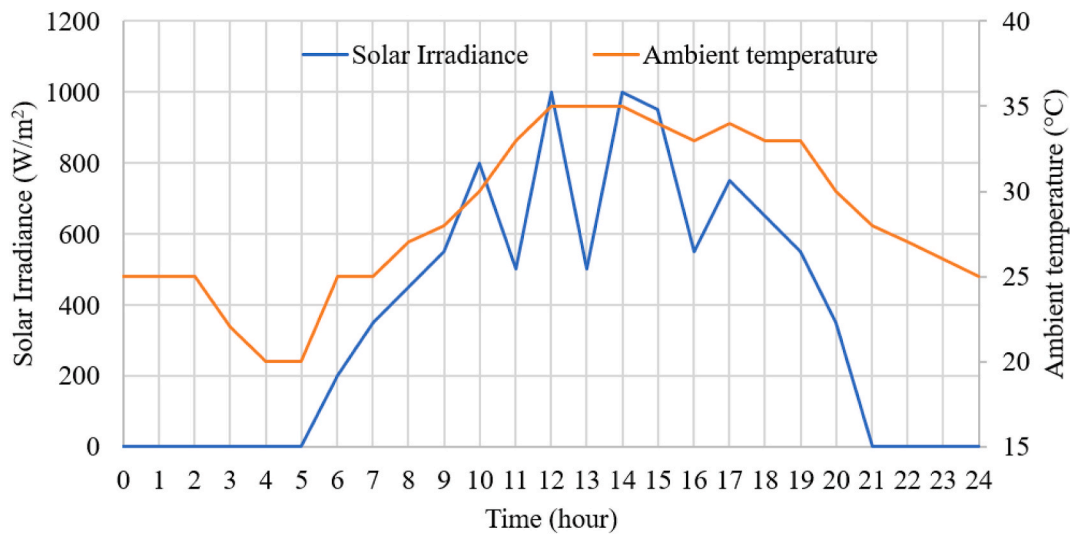


Fig. 9. Solar irradiance and ambient temperature variations profile for the selected day.

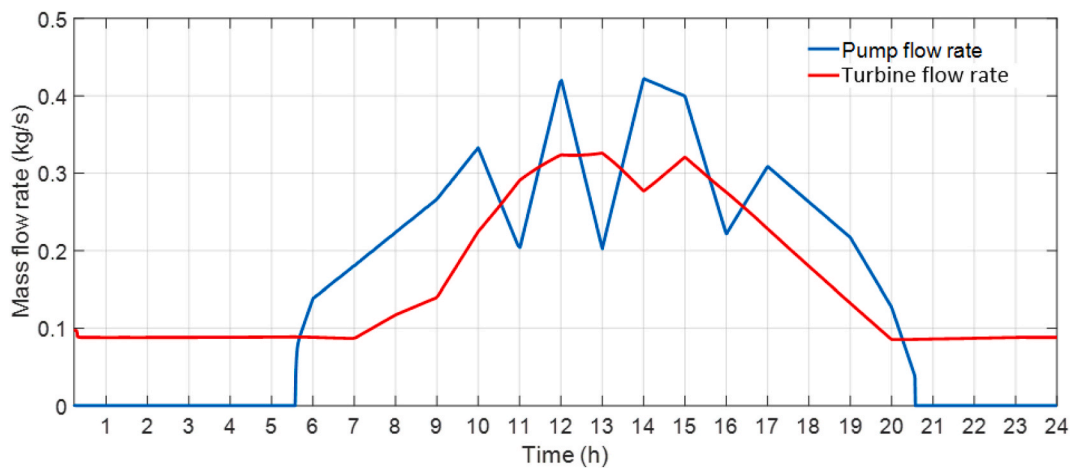


Fig. 10. Variations in the pump and turbine flow rates.

### 5. Results and discussion

In this subsection, the simulation model is built in Simulink\Sim-scape. Influence of solar irradiance and ambient temperature under typical climate conditions are evaluated, afterwards, hourly simulation

for a typical day is conducted. As a design condition, solar irradiance and ambient temperature variation profile in Libya are considered in this study. The rest of the specifications are given in Table 1.

Solar collector array and heat storage dimensions must be calculated and established in order to provide a performance evaluation of the

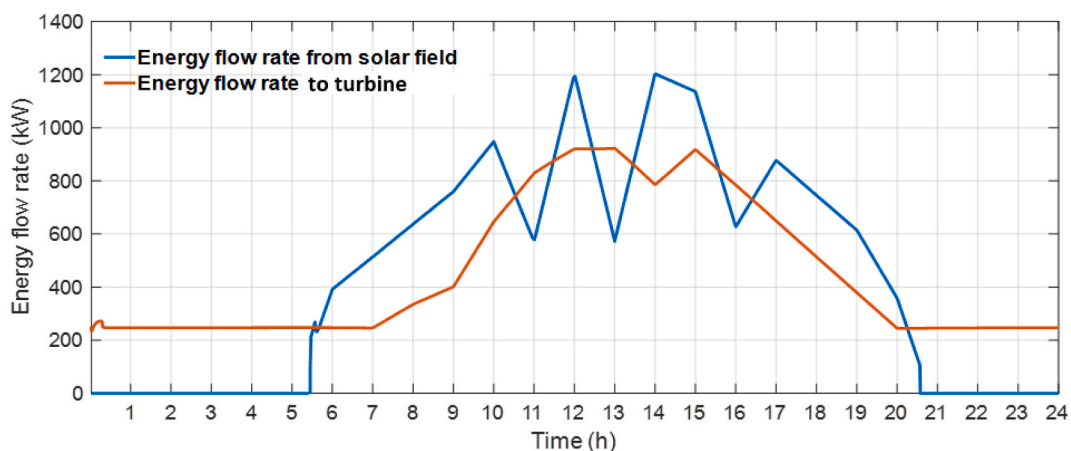


Fig. 11. Variations in the energy flow rate from solar field and to the turbine in selected day.

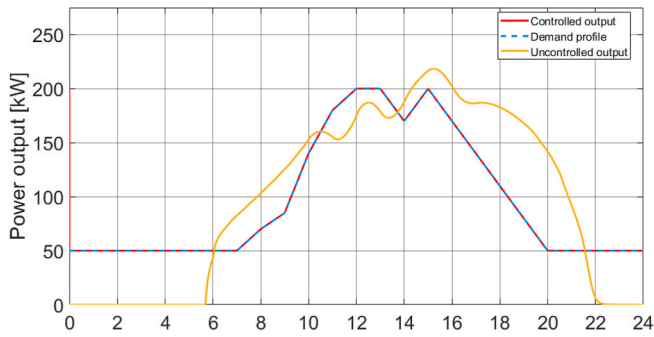


Fig. 12. Variations in the power outputs during the charging and discharging modes on the selected day.

system. As mentioned above a typical day has been selected in this study. Fig. 9 shows selected typical day in March, and it can be notice that there is variation of solar irradiance and ambient temperature levels during the day.

The current system is designed and examined for a hospital in Libya, allowing a solar collector area of 1584 m<sup>2</sup>, which equals 120 collectors, to be chosen. A preliminary evaluation of the system determined that the pressurized steam tank volume should be 160 m<sup>3</sup> as presented in Table 1. The system operation is based on the following strategy: daytime period starts at 07:00, the pump runs, and useful solar heat is collected by the PTC collectors to heat water to be a superheated steam state and stored in the steam accumulator, meanwhile, the turbine generates electricity and supplies hot water to the building. The water flow rate in the solar boiler region is controlled to guarantee only superheated steam goes to the steam accumulator and the throttle valve is adjusted to match electricity demand. Moreover, this prevents excessive use of the heat source. Day time period ends at 20:00 when solar irradiance is not sufficient and night demand period starts. This period covers the main target of the study and ends in the morning. Only Rankine cycle works based on the steam stored in the accumulator and steam flow rate is controlled to satisfy the excessive demand.

Fig. 10 shows the variation of turbine flow rate and circulating water pump flow rate. The blue line presents mass flow rate of the pump, and it's clear to see that this flow rate is fluctuating during the daytime, this fluctuation is because the pump is controlled based on the liquid level in the solar boiler region in order to guarantee only superheated steam goes into the accumulator. As the heat input by the solar field depends on the solar profile, the pump's flow rate is similar to solar irradiance profile during the charging mode. During discharging mode, the pump is off as there is no solar energy. In Fig. 10 the second flow rate is the steam turbine flow rate which is presented by red line, and it is measured after the throttle valve. Since the throttle valve controls the flow of the

turbine inlet, the steam flow rate is controlled according to match the demand. During the discharging mode, the flow rate seems stable at 0.09 kg/s because of the demand is constant and flow is controlled by the valve.

Fig. 11 shows the energy flow rates from the solar field and to the turbine. There are two periods, time one when solar radiation is abundant and another when the system is powered by the steam accumulator. During the discharging mode, the steam accumulator supplies 210 kW of heat energy to run the turbine, to match the demand profile. However, this value during discharging mode seems stable to match energy demand because it is controlled by the throttle valve. The energy flow rate from the solar field is directly affected by the solar irradiance pattern during the day. Thus, it varies by solar irradiance level during the daytime and it is zero when the solar energy is not available during night-time.

Fig. 12 shows electricity demand profile and the system electricity output. Similar patterns can be seen between the system output and the energy demand, where the system control is compelled to generate the necessary electricity. The system is able to meet the hospital's energy needs all day long because the steam accumulator supplies heat at night and during ordinary weather conditions. The orange line in Fig. 12 indicates the power output without control system. The system power generation is zero during the night-time as there is no solar energy and all available heat in the steam accumulator is consumed. As a result of this consumption, pressure in the steam accumulator decreases to the set value and the valve cuts the flow. It shows that using a throttle valve is important to control energy flow rate into the turbine to match the demand.

As control stagey is used by adapting the throttle valve to meet electricity demand profile for the day, Fig. 13 shows dynamic response of the throttle valve area to meet electricity demand. When pressure of the steam is getting lower inside the accumulator, the valve opens to allow more flow rate to go into the turbine to match the demand. In this purpose, the valve area varies during the day considering pressure in the accumulator and the demand.

Fig. 14 shows the thermal efficiency of two regions of solar collectors and the thermal efficiency of the system. The boiler region is the red line, which is higher than the superheat region. As expected, the thermal efficiency of the collectors in the boiler region is higher than the superheating region because of the lower operating temperature. It can be observed that the collector thermal efficiency increases as the solar irradiance increases and decreases with dropping solar irradiance during days with each typical climate condition. Regarding system thermal efficiency, the system has two thermal efficiency periods, one when solar irradiation is available and another when it is not, with the thermal efficiency of the system being 0.20 during the discharging mode and 0.23 during the charging mode.

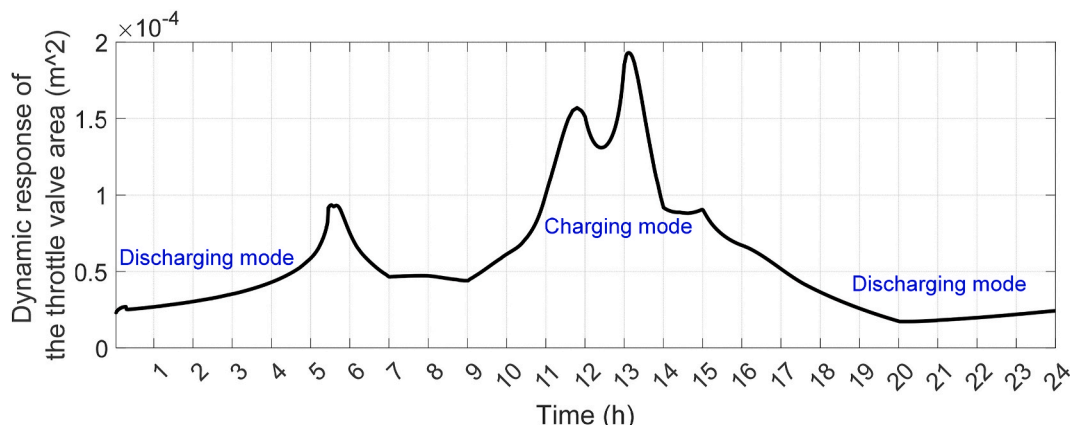


Fig. 13. Dynamic response of the throttle valve opening area to meet the electricity demand for the selected day.

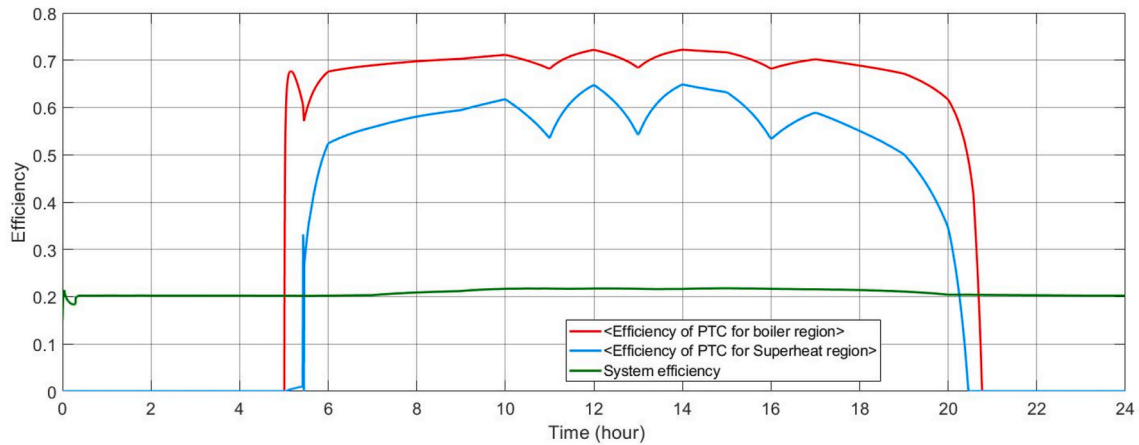


Fig. 14. Variations in thermal efficiency of the solar collector and the whole system.

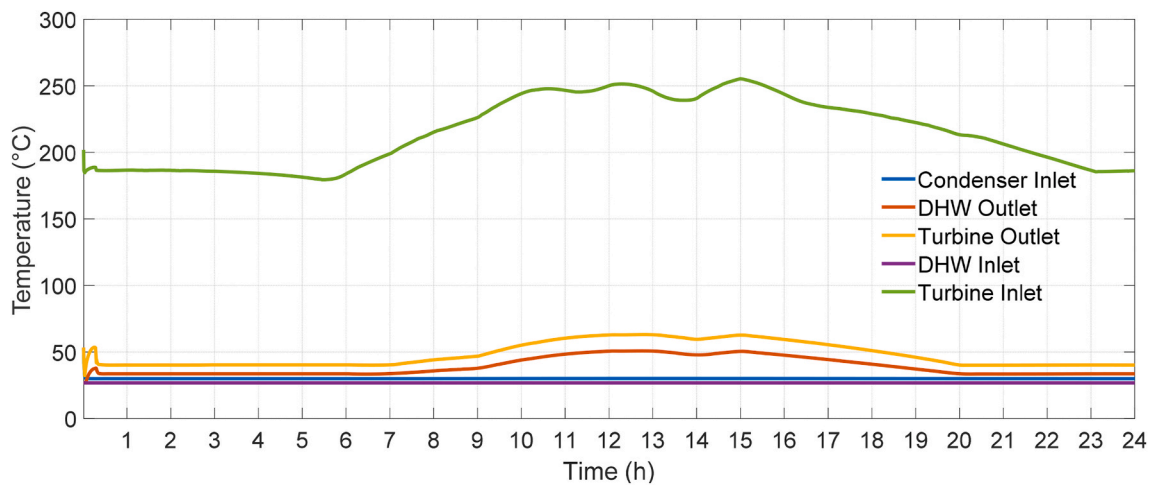


Fig. 15. Variations in the outlet temperature in DHW during the charging and discharging modes.

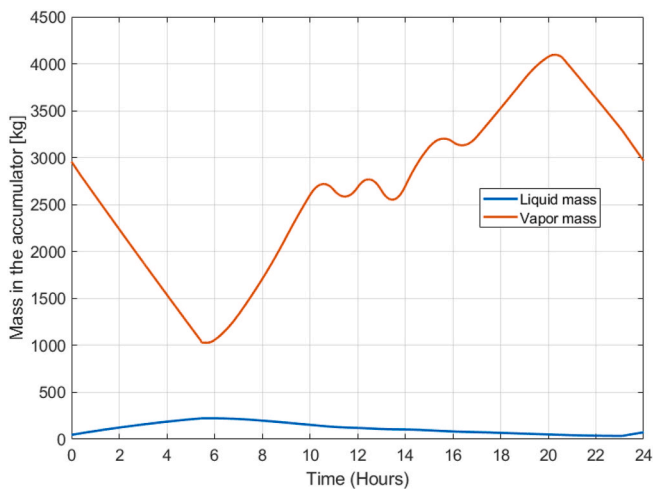


Fig. 16. Variations in the mass of stored vapor and liquid of the steam accumulator.

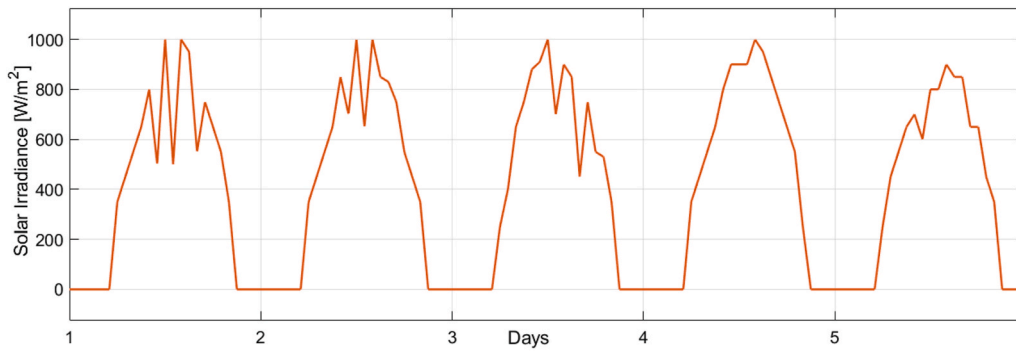
Fig. 15 shows the temperatures of the lines on the DHW side during the day. From 1:00 to 24:00, the outlet hot water temperature reaches up to 52 °C, presented by the red line. The flow rate is kept constant as the hospital requires 4.2 kg/s DHW. The orange line is the inlet turbine

temperature in charging and discharging mode during the day. The blue line indicates a tap source temperature before it enters the DHW system.

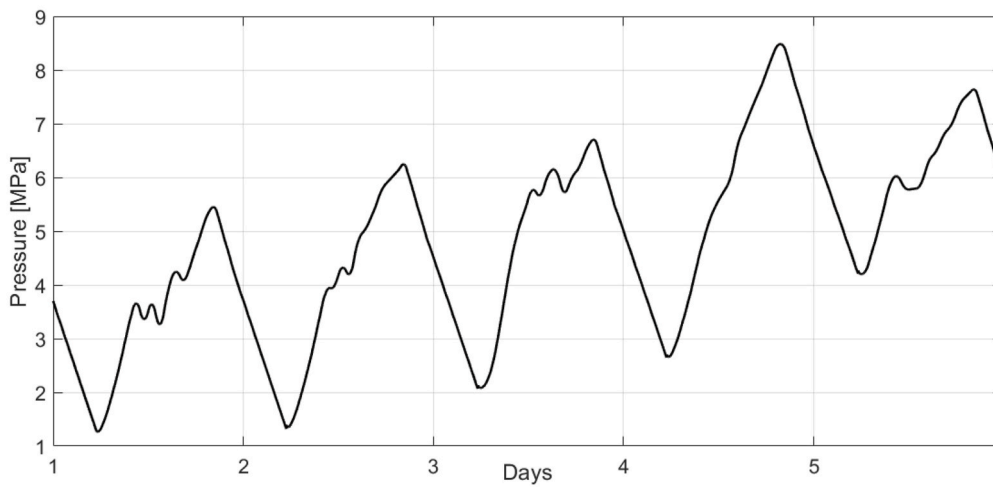
Fig. 16 shows the liquid and vapor masses in the storage during the day. The vapor mass in the accumulator reaches 4000 kg in the evening because the energy is charged in the storage for night operation. Thus, the amount of vapor mass is totally related to solar energy availability and power output of the system. Vapor mass increases in the daytime period due to the good solar radiation level on the day. Due to the lack of steam production at night and the condensed water’s return to the steam accumulator, it appears that the liquid level rises. Steam accumulator’s other purpose is to maintain the system’s safety and prevent the turbine from being harmed because when the fluid at two-phase enters the turbine it may severely damages the turbine blades, causing instability in the system’s output power.

Fig. 17 shows the performance of the system for five days. Firstly, weather data is given in Fig. 17a. The first day is the selected day for one-day simulations, but the remaining days are following real weather data. The system is sensitive to initial conditions for a one-day simulation, however, on consecutive days, the importance of initial conditions is lower. It is good to test the system’s control and its effects on the operating parameters.

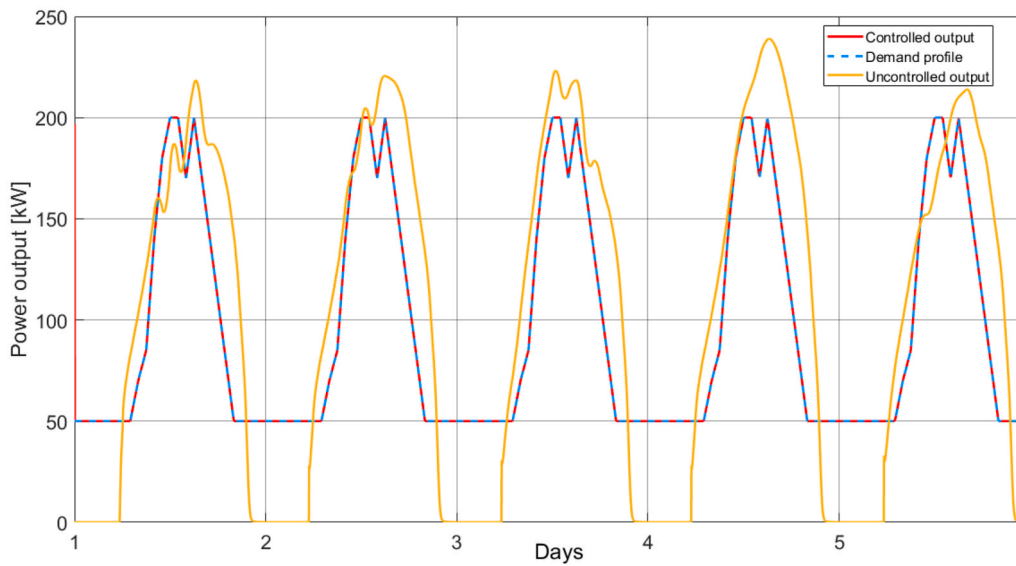
Fig. 17b shows pressure in the steam accumulator for given consecutive days. Since the system is designed to provide the required electricity on a moderate and cloudy day, the advantage of the steam accumulator is seen here. The result of constant power output is seen in the stored steam pressure. Because the second, third and fourth days



a) Solar irradiance data for 5 days



b) Steam accumulator pressure variation for 5 days



c) Power output for controlled and uncontrolled cases

Fig. 17. Variation of solar data, accumulator pressure and power output for five days of operation a) Solar irradiance data for 5 days b) Steam accumulator pressure variation for 5 days c) Power output for controlled and uncontrolled cases.

have better solar irradiance levels despite the constant output, in this way unused energy is stored in the steam accumulator. This stored steam would be used in the day when solar irradiance is not enough to provide the required electricity.

Fig. 17c shows the power outputs of controlled and uncontrolled operations. As the system control is forced to produce the required electricity the trend is quite similar to the energy demand. Thanks to the steam accumulator providing high-pressure steam during solar irradiance variations and during the night, the system can match the energy demand of the hospital throughout the day. It can be seen that the orange line presents uncontrolled system and it is not matching the demand profile, overproduction is observed during day time and the system cannot produce electricity at night as it consumes solar energy.

## 6. Conclusion

In this study, the performance of the direct steam generation solar power system powered by parabolic trough collectors and coupled with a steam accumulator as a heat storage unit and also a domestic hot water (DHW) system to meet the electricity and hot water requirements of a Libyan hospital was dynamically simulated via using Simulink\Simscape software. The system was designed and evaluated by controlling the inlet pressure of the steam turbine and also the flow rate of water circulation pump. The main conclusions can be drawn as follows.

- With using a steam accumulator and controlling the inlet pressure of turbine, the power out of the DSG solar power system can match the electricity demand profile of a hospital under typical Libyan climate conditions.
- The thermal efficiency of system reached to 0.23 when solar irradiance is the highest at the noon and 0.20 when the system works with only the stored steam from the steam accumulator.
- Simulink\Simscape is a convenient superior tool in constructing the model of advanced solar power system and simulating its dynamic performance over a long period.

## CRedit authorship contribution statement

**Amin Ehtiwesh:** Investigation, Software, Writing – original draft. **Cagri Kutlu:** Investigation, Writing – original draft. **Yuehong Su:** Conceptualization, Writing – review & editing, Supervision. **Saffa Rif-fat:** Supervision.

## Declaration of competing interest

The authors declare that they have no known competing financial interests or personal relationships that could have appeared to influence the work reported in this paper.

## Data availability

The authors are unable or have chosen not to specify which data has been used.

## Acknowledgments

The first author would like to thank the General Electric Company of Libya and the Libyan ministry of higher education for providing information of electricity demand and information maps of the country.

## References

- [1] J. Li, P. Li, G. Pei, J.Z. Alvi, J. Ji, Analysis of a novel solar electricity generation system using cascade Rankine cycle and steam screw expander, *Appl. Energy* 165 (2016) 627–638.
- [2] M.A. Mousa, I.M. Saleh, M. Molokhia, COMPARATIVE STUDY IN SUPPLYING ELECTRICAL ENERGY TO SMALL REMOTE LOADS IN LIBYA, 1998.

- [3] A.M.A. Mohamed, A. Al-Habaibeh, H. Abdo, S. Elabar, Towards exporting renewable energy from MENA region to Europe: an investigation into domestic energy use and householders' energy behaviour in Libya, *Appl. Energy* 146 (2015) 247–262.
- [4] J. Soares, A.C. Oliveira, L. Valenzuela, A dynamic model for once-through direct steam generation in linear focus solar collectors, *Renew. Energy* 163 (2021) 246–261.
- [5] D. Lei, X. Fu, Y. Ren, F. Yao, Z. Wang, Temperature and thermal stress analysis of parabolic trough receivers, *Renew. Energy* 136 (2019) 403–413.
- [6] M. Eck, W.D. Steinmann, Direct steam generation in parabolic troughs: first results of the DISS project, *J. Solar Energy Eng., Trans. ASME* 124 (2002) 134–139.
- [7] E. Zarza, L. Valenzuela, J. León, et al., The DISS Project: direct steam generation in parabolic trough systems. operation and maintenance experience and update on project status, *J. Solar Energy Eng., Trans. ASME* 124 (2002) 126–133.
- [8] M. Alguacil, C. Prieto, A. Rodriguez, J. Lohr, Direct steam generation in parabolic trough collectors, *Energy Procedia, Elsevier Ltd* (2014) 21–29.
- [9] E. Zarza, M.E. Rojas, L. González, J.M. Caballero, F. Rueda, INDITEP: the first pre-commercial DSG solar power plant, *Sol. Energy* 80 (2006) 1270–1276.
- [10] S. Sallam, M. Taqi, Analysis of direct steam generation in parabolic trough solar collectors under hot climate, *Appl. Therm. Eng.* (2023) 219.
- [11] T. Suwa, Transient heat transfer performance prediction using a machine learning approach for sensible heat storage in parabolic trough solar thermal power generation cycles, *J. Energy Storage* 56 (2022).
- [12] O. Behar, A. Khellaf, K. Mohammedi, A review of studies on central receiver solar thermal power plants, *Renew. Sustain. Energy Rev.* 23 (2013) 12–39.
- [13] J.E. Hoffmann, E.P. Dall, Integrating desalination with concentrating solar thermal power: a Namibian case study, *Renew. Energy* 115 (2018) 423–432.
- [14] A.G. Fernández, J. Gomez-Vidal, E. Oro, A. Kruiženga, A. Solé, L.F. Cabeza, Mainstreaming commercial CSP systems: a technology review, *Renew. Energy* 140 (2019) 152–176.
- [15] L. Li, J. Sun, Y. Li, Y.L. He, H. Xu, Transient characteristics of a parabolic trough direct-steam-generation process, *Renew. Energy* 135 (2019) 800–810.
- [16] C. Kutlu, J. Li, Y. Su, G. Pei, S. Riffat, Off-design performance modelling of a solar organic Rankine cycle integrated with pressurized hot water storage unit for community level application, *Energy Convers. Manag.* 166 (2018) 132–145.
- [17] Z. Aghaziarati, A.H. Aghdam, Thermoeconomic analysis of a novel combined cooling, heating and power system based on solar organic Rankine cycle and cascade refrigeration cycle, *Renew. Energy* 164 (2021) 1267–1283.
- [18] E.A. Pina, M.A. Lozano, L.M. Serra, A. Hernández, A. Lázaro, Design and thermoeconomic analysis of a solar parabolic trough – ORC – biomass cooling plant for a commercial center, *Sol. Energy* 215 (2021) 92–107.
- [19] A. Arteconi, L. del Zotto, R. Tascioni, L. Cioccolanti, Modelling system integration of a micro solar Organic Rankine Cycle plant into a residential building, *Appl. Energy* (2019) 251.
- [20] J. Li, P. Li, G. Gao, G. Pei, Y. Su, J. Ji, Thermodynamic and economic investigation of a screw expander-based direct steam generation solar cascade Rankine cycle system using water as thermal storage fluid, *Appl. Energy* 195 (2017) 137–151.
- [21] A.O.M. Maka, S. Salem, M. Mehmood, Solar photovoltaic (PV) applications in Libya: challenges, potential, opportunities and future perspectives, *Clean. Eng. Technol.* 5 (2021).
- [22] P. Li, J. Li, G. Gao, et al., Modeling and optimization of solar-powered cascade Rankine cycle system with respect to the characteristics of steam screw expander, *Renew. Energy* 112 (2017) 398–412.
- [23] A. Ehtiwesh, C. Kutlu, Y. Su, J. Darkwa, Comparison of direct steam generation and indirect steam generation of solar rankine cycles under Libyan climate conditions, in: *Advances in Heat Transfer and Thermal Engineering*, Springer, Singapore, 2021, pp. 785–790.
- [24] S.A. Kalogirou, Solar thermal collectors and applications, *Prog. Energy Combust. Sci.* 30 (2004) 231–295.
- [25] G. Gao, J. Li, P. Li, et al., Design of steam condensation temperature for an innovative solar thermal power generation system using cascade Rankine cycle and two-stage accumulators, *Energy Convers. Manag.* 184 (2019) 389–401.
- [26] S. Zhang, M. Liu, Y. Zhao, K. Zhang, J. Liu, J. Yan, Thermodynamic analysis on a novel bypass steam recovery system for parabolic trough concentrated solar power plants during start-up processes, *Renew. Energy* 198 (2022) 973–983.
- [27] R. Wang, J. Sun, H. Hong, Proposal of solar-aided coal-fired power generation system with direct steam generation and active composite sun-tracking, *Renew. Energy* 141 (2019) 596–612.
- [28] A. Orumiyehi, M. Ameri, M.H. Nobakhti, M. Zareh, S. Edalati, Transient simulation of hybridized system: waste heat recovery system integrated to ORC and Linear Fresnel collectors from energy and exergy viewpoint, *Renew. Energy* 185 (2022) 172–186.
- [29] V.D. Stevanovic, M.M. Petrovic, S. Milivojevic, B. Maslovaric, Prediction and control of steam accumulation, *Heat Tran. Eng.* 36 (2015) 498–510.
- [30] Mathworks, Local Restriction (2P), 2022. <https://uk.mathworks.com/help/simscape/ref/localrestriction2p.html>. (Accessed 25 January 2023).
- [31] G. Gao, J. Li, P. Li, H. Yang, G. Pei, J. Ji, Design and analysis of an innovative concentrated solar power system using cascade organic Rankine cycle and two-tank water/steam storage, *Energy Convers. Manag.* (2021) 237.
- [32] L. Willwerth, J.F. Feldhoff, D. Krüger, et al., Experience of operating a solar parabolic trough direct steam generation power plant with superheating, *Sol. Energy* 171 (2018) 310–319.
- [33] Agora Energiewende, Flexibility in Thermal Power Plants - with a Focus on Existing Coal-fired Power Plants, Prognos AG and Fichtner GmbH & Co, 2022 (KG Report, 115/04-S-2022/EN).

- [34] C. Tiba, V.W. Bezerra Azevedo, M.D.A.C. Paes, LFL de Souza, Mapping the potential for a combined generation of electricity and industrial process heat in the northeast of Brazil - case study: bahia, *Renew. Energy* 199 (2022) 672–686.
- [35] X. Cui, K.J. Chua, M.R. Islam, W.M. Yang, Fundamental formulation of a modified LMTD method to study indirect evaporative heat exchangers, *Energy Convers. Manag.* 88 (2014) 372–381.
- [36] A. Naminezhad, M. Mehregan, Energy and exergy analyses of a hybrid system integrating solar-driven organic Rankine cycle, multi-effect distillation, and reverse osmosis desalination systems, *Renew. Energy* 185 (2022) 888–903.
- [37] EnergyPlus. Weather data. <https://energyplus.net/weather/>. (Accessed 30 October 2019).